



Salt Precipitation Law of Formation Water During CO₂ Injection into Depleted Gas Reservoirs

Yu Yang¹, Qi-lin Xu²(✉), Liang-wei Jiang¹, Qian Zhang³, Dong-jie Huang⁴, Xin Liu³, Rong-he Liu⁵, Jian-guo Liu⁶, and Yu-zhe Cui⁷

¹ College of Energy, Chengdu University of Technology, Chengdu, China

² Shixi Oilfield Operation Area, Xinjiang Oilfield Company, Karamay, China
2207128878@qq.com

³ Hainan Branch of CNOOC Co., Ltd., Haikou, China

⁴ Sichuan Institute of Nonmetallic (Salt Industry) Geological Survey, Zigong, China

⁵ CNPC Chuanqing Drilling Engineering Co., Ltd., Chengdu, China

⁶ Tianjin Branch of CNOOC Co., Ltd., Tianjin, China

⁷ Exploration and Development Research Institute of Liaohe Oilfield Company, Panjin, China

Abstract. After CO₂ is injected into the formation, some CO₂ will dissolve in the formation water and react with rocks, changing the ion type and content of the formation water, accompanied by water evaporation and salting out. Taking a depleted gas reservoir in the west Sichuan Basin as an example, CMG simulation software was applied to simulate the gas, water and solid phase equilibrium in the process of CO₂ injection, based on the PR Henry equation, water-rock reaction kinetics theory, and salting out model. Research showed that: ① During the injection process of CO₂, water evaporation caused a gradual decrease in the formation water saturation, leading to a gradual increase in the salinity of the formation water. However, because the small change in water saturation, the increase in salinity of formation water wasn't significant; ② Water evaporation reduces the water saturation of the formation, confirming an increase in the mole number of H₂O component in the gas phase. However, because the mole number of CO₂ component in the gas phase increases faster, the mole fraction of H₂O component in the gas phase still continues to decline; ③ With the gradual increase of CO₂

Copyright 2023, IFEDC Organizing Committee.

This paper was prepared for presentation at the 2023 International Field Exploration and Development Conference in Wuhan, China, 20–22 September 2023.

This paper was selected for presentation by the IFEDC Committee following review of information contained in an abstract submitted by the author(s). Contents of the paper, as presented, have not been reviewed by the IFEDC Technical Team and are subject to correction by the author(s). The material does not necessarily reflect any position of the IFEDC Technical Committee its members. Papers presented at the Conference are subject to publication review by Professional Team of IFEDC Technical Committee. Electronic reproduction, distribution, or storage of any part of this paper for commercial purposes without the written consent of IFEDC Organizing Committee is prohibited. Permission to reproduce in print is restricted to an abstract of not more than 300 words; illustrations may not be copied. The abstract must contain conspicuous acknowledgment of IFEDC. Contact email: paper@ifedc.org.

© The Author(s), under exclusive license to Springer Nature Singapore Pte Ltd. 2024

J. Lin (Ed.): IFEDC 2023, SSGG, pp. 325–342, 2024.

https://doi.org/10.1007/978-981-97-0268-8_27

solubility, calcite which belongs to the carbonate mineral and anorthite, k-feldspar belong to the feldspar mineral were dissolved, kaolinite and illite which belong to the clay mineral were precipitated; ④ Due to the combined action of water-rock reaction and salt-out, the content of OH⁻ ions in water gradually decreases and the content of H⁺, Ca²⁺, HCO₃⁻, Al³⁺, SiO₂(aq) ions continuously increases; ⑤ During the CO₂ injection process, the precipitation of CaSO₄, CaSO₄ · 2H₂O were inhibited, and CaCO₃ was the main precipitation product. The research results have certain reference significance for the study of the salt-out law of formation water during the geological storage process of CO₂ in depleted gas reservoirs.

Keywords: CO₂ Injection · Depleted Gas Reservoir · Formation Water Evaporation · Water Rock Reaction · Salt Precipitation

With the development of the economy, human industrial production, and life in large quantities of fossil fuels, resulting in a sudden increase in carbon dioxide emissions, the resulting greenhouse effect has seriously threatened the survival of the human environment. Carbon dioxide capture and storage is an effective way to reduce carbon dioxide emissions [1]. Depleted gas reservoirs are ideal places for CO₂ geological sequestration. Therefore, CO₂ geological sequestration of depleted gas reservoirs has gradually become a research hotspot nowadays [2].

During the development and gas injection processes of gas reservoirs, salt-out phenomena occur [3, 4]. In the process of gas reservoir development, with the decrease of formation pressure, the boiling point of water decreases, and the mole fraction of water in the gas phase increases gradually, resulting in the salting-out phenomenon [5, 6]. However, in the process of CO₂ injection, the formation pressure rises and the salting-out phenomenon still occurs. Zhang et al. confirmed that CO₂ injection would lead to the precipitation of CaSO₄ and NaCl through the experiment of CO₂ injection in the brine layer [7]. Peysson et al. confirmed the phenomenon of water evaporation and salting out by injecting nitrogen into consolidated sandstone cores, which would lead to the reduction of core injection capacity [8]. In the continuous injection and production process of gas storage, water evaporation and salting out will affect the normal operation of gas storage [9–11]. Many factors affect formation salting out, such as temperature changes, pressure changes, etc. Wang Chunyan et al. [12] summarized the mechanism of salting-out formation in the continuous injection and production process of gas storage based on the principles of salting-out thermodynamics and salting-out crystallization dynamics. Morin and Montel [13] believed that salting-out was caused by mass transfer when they studied the causes of NaCl precipitation in strata.

Although scholars at home and abroad have carried out many studies on the salt-out mechanism in the process of gas injection, the following two scientific problems still exist in the process of CO₂ injection in depleted gas reservoirs: ① When domestic and foreign scholars analyze CO₂ geological storage, the formation water of the research object is generally equivalent to NaCl formation water [14–17]. However, the formation water of depleted gas reservoirs is mostly CaCl₂ type, and is there a difference in its salting out pattern compared to NaCl type formation water? ② The CO₂ injection process is accompanied by the occurrence of CO₂ dissolution, mineral dissolution and precipitation, and water evaporation. What are the effects of these three factors on salt

precipitation? Therefore, it is necessary to use numerical simulation methods to study the evaporation and salting out laws of the formation water during CO₂ injection in depleted gas reservoirs.

1 Phase Equilibrium Model During CO₂ Injection

The gas state equation is a function that characterizes the relationships between gas temperature, pressure, density, etc. [18]. The PR equation of state and Henry's law proposed by Li and Nghiem [19] can accurately describe the thermodynamic equilibrium of CO₂ water. Based on the chemical equilibrium equation, reaction kinetics equation, and saturation index theory, the laws of mineral dissolution, precipitation, and salting out are analyzed.

1.1 Equation of State for a Gas

Using the PR equation of state combined with Henry's law, the solubility of CO₂ and evaporation of water can be calculated under different (P, T) conditions. The expression of the PR equation of state is [20]:

$$P = \frac{RT}{(V_m - b)} - \frac{a}{V_m(V_m + b) + b(V_m - b)} \quad (1)$$

where, P is the system pressure, MPa; V_m is the molar volume, cm³/mol; R is the universal gas constant, usually 8.314, J/(mol·K); T is the system temperature, K; a and b are the equation of state parameters, dimensionless.

For mixtures, the following mixing rules are generally used:

$$a = \sum_i \sum_j x_i x_j a_{ij} \quad (2)$$

$$b = \sum_i x_i b_i \quad (3)$$

where:

$$a_{ij} = (1 - \delta_{ij}) a_i^{1/2} a_j^{1/2} \quad (4)$$

$$a_i = a_i(T_{Ci}) \alpha_i(T_{ri}, \omega_i) \quad b_i = \frac{0.07796RT_{Ci}}{p_{Ci}} \quad (5)$$

$$a_i(T_{Ci}) = \frac{0.45724R^2T_{Ci}^2}{p_{Ci}} \quad (6)$$

where, δ_{ij} is the binary interaction factor of component i and component j , dimensionless; x_i is the mole fraction of component i , dimensionless; x_j is the mole fraction of j component, dimensionless; p_{Ci} is the critical pressure, MPa; T_{Ci} is critical temperature,

K ; Z_{Ci} is the critical compression factor of gas, dimensionless; a_i, b_i is the equation of state parameter of component i pure substance, dimensionless.

According to the laws of thermodynamics, the following is true

$$\ln \frac{f}{p} = \int_0^p \left(\frac{V_m}{RT} - \frac{1}{p} \right) dp \quad (7)$$

where, f is the fugacity of gas component, MPa.

The fugacity coefficient of component i is derived from Eqs. (2) and (3)

$$\ln \left(\frac{f_i}{x_i p} \right) = \frac{b_i}{b} (Z - 1) - \ln(Z - B) - \frac{A}{2\sqrt{2}B} \left(\frac{2 \sum_j x_j a_{ij}}{a} - \frac{b_i}{b} \right) \ln \left(\frac{Z + 2.414B}{Z - 0.414B} \right) \quad (8)$$

where, $\frac{f_i}{x_i p}$ is the fugacity coefficient of component i , dimensionless; Z is the gas compression factor, dimensionless; A and B are both constants, $A = \frac{ap}{(RT)^2}$, $B = \frac{bp}{RT}$, dimensionless.

The fugacity of components in the gas phase was calculated by the PR equation of state and in the water phase by Henry's law. According to Henry's law, the fugacity of the soluble gas phase i component in the water phase can be expressed as

$$f_{iw} = y_{iw} \cdot H_i \quad (9)$$

where, f_{iw} is the fugacity of component i in the water phase, MPa; y_{iw} is the mole fraction of component i in the water phase, dimensionless; H_i is the Henry constant of component i , which is related to temperature, pressure and salinity, MPa.

According to the different temperature and pressure, the Henry constant can be calculated by the following formula:

$$\ln H_i = \ln H_i^* + v_i^\infty p / RT \quad (10)$$

where, H_i^* is the Henry constant of component i under reference temperature and pressure; v_i^∞ is the partial molar volume, cm^3/mol , which can be calculated by the relevant empirical formula.

Henry constant under different formation of water salinity can be calculated by the following formula [21]:

$$\log_{10} \left(\frac{H_{salt,i}}{H_i} \right) = k_{salt,i} m_{salt} \quad (11)$$

where, $H_{salt,i}$ is the Henry constant of component i under the corresponding salinity; H_i is the Henry constant of component i under pure water condition; $k_{salt,i}$ is the correlation coefficient between component i and salinity, which can be calculated by relevant empirical formula without dimensionality; m_{salt} is the salinity of formation water, mol/kg.

According to the thermodynamic equilibrium theory, the following formula should be true when the system is in phase equilibrium:

$$f_i^v = f_i^w \quad (12)$$

where, f_i^v is the fugacity of component i in the gas phase; f_i^w is the fugacity of component i in the water phase.

At present, the PR-Henry equation has been used to calculate gas-liquid equilibrium, which can be calculated by Newton-Raphson's iterative method. The main steps are as follows [22]:

- (1) Input the system temperature, pressure, molar composition of the mixture, and critical parameters of each component, and estimate the initial value of the gas-liquid phase composition based on Wilson's formula;
- (2) Calculate the equation of state parameters for the mixture;
- (3) Calculate the molar composition of each component in the gas-liquid phase, and then obtain the corresponding fugacity coefficient;
- (4) Compare whether the gas-liquid phase fugacity difference is less than the error value. If so, output equilibrium pressure, and molar composition of each component in the gas-liquid phase; Otherwise, re-estimate the initial value of the gas-liquid phase composition and return to step (2) to recalculate.

1.2 Mechanism of CO₂ Dissolution and Water-Rock Reaction

1.2.1 Type of Water-Rock Reaction

Formation water in gas reservoirs usually contains Na⁺, K⁺, Ca²⁺, Mg²⁺, Cl⁻, SO₄²⁻ and HCO₃⁻ ions, and contains six salt components: CaCO₃, CaSO₄, CaSO₄·2H₂O, NaCl, KCl and Mg(OH)₂. Some of the CO₂ injected will dissolve in the formation water and react with the rock, changing the type and content of ions in the formation water.

Two-stage ionization exists in carbonic acid generated after CO₂ is dissolved in formation water, and ionization reaction also exists in water [23]:



For H₂CO₃, two-stage ionization will increase the concentration of CO₃²⁻ and correspondingly change the concentration of Ca²⁺ in equilibrium with CaCO₃, which will affect the chemical equilibrium of CaCO₃, CaSO₄·2H₂O and CaSO₄ in formation water. K_a is assumed to be the equilibrium constant of H₂CO₃ ionization, and K_b is the equilibrium constant of HCO₃⁻ ionization, which is defined as:

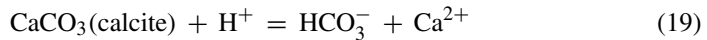
$$K_a = \frac{[\text{H}^+][\text{HCO}_3^-]}{[\text{H}_2\text{CO}_3]} \quad (17)$$

$$K_b = \frac{[H^+][CO_3^{2-}]}{[HCO_3^-]} \quad (18)$$

The ionization of carbonic acid will make the formation water appear weak acid, resulting in the dissolution and precipitation of rock minerals in the reservoir. Minerals can be divided into carbonate minerals, feldspar minerals, and clay minerals according to mineral composition and rock structure.

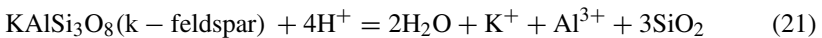
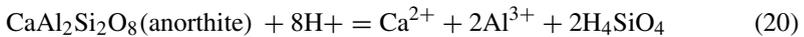
(1) Carbonate minerals

Carbonate minerals mainly include calcite, dolomite, magnesite, siderite, and so on. Calcite and dolomite have faster dissolution/precipitation rates, followed by siderite and the lowest magnesite [24]. The reaction sensitivity of calcite and dolomite is higher under the action of CO₂ fluid. The calcite dissolution reaction is shown as follows:



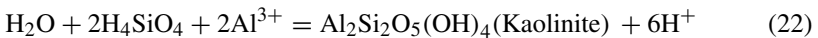
(2) Feldspar minerals

Feldspar is one of the important rock-forming minerals in silicate salt minerals containing sodium, potassium, and calcium in strata rocks [25]. Feldspar mineral category more, according to the composition of elements can be divided into calcium feldspar, potassium feldspar, and so on. Compared with potassium feldspar, calcium feldspar has higher sensitivity. The dissolution reaction of anorthite and potassium feldspar is shown as follows:



(3) Clay minerals

Clay minerals are water-containing aluminosilicate minerals with a layered structure, which are the main mineral components of clay rocks. Clay minerals include kaolinite, illite, plagioclhorite, montmorillonite, etc. The dissolution/precipitation rates of plagioclhorite are relatively high, while those of illite, kaolinite, and montmorillonite are relatively low. The kaolinite precipitation reaction is shown as follows:



1.2.2 Hydrodynamic Equation of the Water-Rock Reaction

Based on the principle of chemical kinetics, the reaction rate of mineral dissolution and precipitation can be expressed as [26]:

$$r_\beta = \hat{A}_\beta k_\beta \left(1 - \frac{Q_\beta}{K_{eq,\beta}} \right), \beta = 1, \dots, R_{mm} \quad (23)$$

where, r_β is the chemical reaction rate, mol/(m³·s); \hat{A}_β is the specific surface area of mineral reaction, m²/m³; k_β is the reaction rate constant of mineral β , mol/(m²·s); $K_{eq,\beta}$ is the reaction equilibrium constant of mineral β ; Q_β is the coefficient related to ion activity in mineral β dissolution reaction, $Q_\beta = \prod_{i=1}^{n_{aq}} a_i^{v_{i\beta}}$; a_i is the activity of component i in mineral β dissolution reaction; $v_{i\beta}$ is the chemical reaction measurement number of component i , when the mineral β dissolution and precipitation reach equilibrium, $Q_\beta = K_{eq,\beta}$.

The chemical reaction rate constant can be calculated by the transition state theory, in which it can be expressed as [27]:

$$k_0 = k_0^* \cdot \exp\left[-\frac{E_a}{R}\left(\frac{1}{T} - \frac{1}{T^*}\right)\right] \quad (24)$$

where, k_0 is the chemical reaction rate constant, mol/(m²·s); k_0^* is the standard rate constant at the reference temperature; E_a is the reaction activation energy, J/mol; R is the universal gas constant, J/(mol·K), usually 8.314; T^* is the reference temperature, usually 298K; T is the system temperature, K.

1.3 Salting-Out Model

The injected CO₂ dissolves in the formation water and reacts with the rock, changing the type and content of ions in the formation water. At the same time, the injected dry CO₂ will cause evaporation of the formation water. Under the combined action of the two, the ion content of formation water changes, and the salinity of formation water increases, so that the saturation index of some salt components in formation water is greater than zero, and the salting-out phenomenon occurs.

At present, the saturation index method is the most used method for the judgment and study of the salt composition relative to the groundwater saturation state [28]. Saturation Indices are defined as follows:

$$SI = \lg(IAP/K_{sp}) \quad (25)$$

where, K_{sp} is the equilibrium constant of the dissolution reaction of salt components; IAP is the activity product of related ions in the dissolution reaction of salt components.

According to the solubility product rule:

- ① When $SI > 0$, salt components precipitate in groundwater;
- ② When $SI = 0$, the dissolution, and precipitation of salt components reach equilibrium;
- ③ When $SI < 0$, the salt component in groundwater is in an unsaturated state, and the salt component tends to dissolve.

Assuming that an independent chemical reaction occurs in the system, the chemical reaction can be expressed as follows:



When the reaction (8) is in an equilibrium state, the equilibrium constant K is expressed as:

$$K = \frac{a_C^{v_C} a_D^{v_D}}{a_A^{v_A} a_B^{v_B}} \quad (27)$$

where, K is the reaction equilibrium constant, a_A , a_B , a_C , a_D which is the concentration of components A, B, C, and D when they are in equilibrium.

According to thermodynamic theory, the reaction equilibrium constant can be calculated from the standard Gibbs free energy of chemical reactions. The formula is as follows:

$$\lg K = \frac{-\Delta G_R^\ominus}{2.303RT} \quad (28)$$

where, ΔG_R^\ominus is the standard Gibbs free energy of the chemical reaction, kJ/mol.

When the temperature is not equal to 298.15K, the variation of the chemical reaction equilibrium constant with temperature can be calculated according to the Van't Hoff formula. If ΔH_R^\ominus is not related to temperature or the temperature variation range is relatively small, within this temperature range, ΔH_R^\ominus can be treated as a constant approximately. According to the Van' t Hoff formula, under constant pressure conditions, there are:

$$\ln K = \ln K_1 + \frac{\Delta H_R^\ominus}{R} \left(\frac{1}{T_1} - \frac{1}{T} \right) \quad (29)$$

where, K_1 is the equilibrium constant of the reaction at 25 °C, and ΔH_R^\ominus is the standard enthalpy change of the reaction, kJ/mol.

1.4 Three-Phase Balance Analysis Process

To analyze the effect of CO₂ dissolution on the salt formation of CaCO₃, CaSO₄·2H₂O, and CaSO₄, the calculation steps are as follows:

- ① Calculate the solubility of CO₂ based on the SRK-HV equation of state;
- ② Calculate the K_a and K_b values at room temperature according to formulas (17), (18), and (24), and then calculate the K_a and K_b values at corresponding temperatures according to Van't Hoff formula (29), thereby obtaining the HCO₃⁻ content at different CO₂ solubility;
- ③ Based on the existing formation water ion content and calculated HCO₃⁻ content data, and based on the saturation index theory in the salt out model, the saturation indexes of CaCO₃, CaSO₄·2H₂O, and CaSO₄ can be calculated for different CO₂ solubility, and then the impact of CO₂ dissolution on the three types of salt formation can be analyzed.

After the change of gas-liquid equilibrium, mineral dissolution/precipitation, and formation water ion content was determined by numerical simulation, the salting-out law was analyzed in combination with the salting-out model. The simulation process is shown in Fig. 1 below.

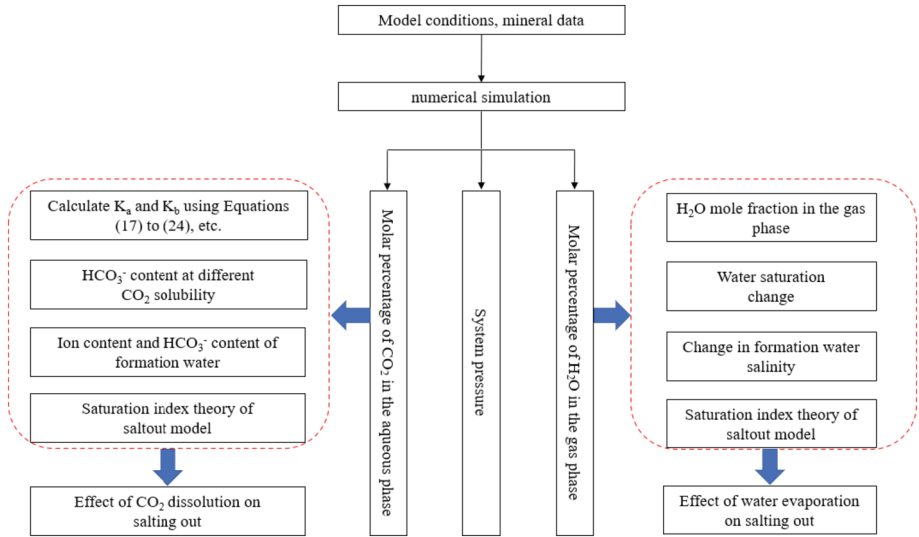


Fig. 1. Simulation flow chart

2 Simulation Example of Water Evaporation and Salting Out During CO₂ Injection

For the CO₂ injection process in depleted gas reservoirs, phase equilibrium and salt out models are used to calculate the system pressure under different CO₂ mole numbers, and obtain the CO₂ solubility, water evaporation, and formation water salinity under different system pressures; In addition, calculate the saturation index of salt components under different mineralization degrees, and analyze the formation water evaporation rule, salt out type, and salt out trend during CO₂ injection.

2.1 Simulation Establishment

In the process of CO₂ injection in depleted gas reservoirs, the range and degree of influence of CO₂ injection temperature on the reservoir temperature are small due to the large reservoir depth and high formation temperature, so the CO₂ injection process can be regarded as a constant temperature process. In this study, CO₂ injection into the gas zone of the gas reservoir was simulated. CMG numerical simulation software was used to establish a $20 \times 1 \times 1$ grid model with a grid step size of $50 \times 20 \times 20$ m. The model was shown in Fig. 2. The continuous injection was set for 5 years and the injection well injection rate was 3000 m³/d.

This paper takes the geological characteristics of a depleted gas reservoir in western Sichuan as an example, and the basic parameters of the model are shown in the Table 1 below [29, 30].

The original components of the model fluid are CH₄, CO₂, and H₂O, and the fluid composition is shown in Table 2. Under the conditions of initial pressure (6 MPa) and temperature (94.3 °C), calculated based on flash equilibrium:

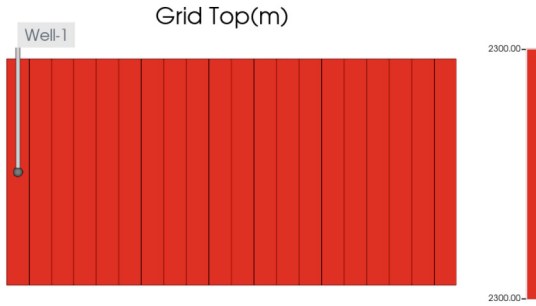


Fig. 2. Grid model

Table 1. Model parameters

Parameter	Value	
Formation parameter	Reservoir temperature (°C)	94.3
	Reservoir pressure (MPa)	6
	Porosity (%)	10
	Permeability (mD)	25
	Connate water saturation S_{wr}	35%
	Thickness (m)	20
	Reservoir top depth (m)	2300
Relative permeability	Liquid phase [31]	$k_{rw} = \sqrt{\frac{S_w - S_{wr}}{1 - S_{wr}}} \left[1 - \left(1 - \left(\frac{S_w - S_{wr}}{1 - S_{wr}} \right)^{\frac{1}{\lambda}} \right)^{\lambda} \right]^2$
	Connate water saturation S_{wr}	0.35
	Index λ	0.58
	Gas phase [32]	$k_{rg} = \left(1 - \frac{S_w - S_{wr}}{1 - S_{wr} - S_{gr}} \right)^2 \left(1 - \left[\frac{S_w - S_{wr}}{1 - S_{wr} - S_{gr}} \right]^2 \right)$
	Residual gas saturation S_{gr}	0.2

① In the gas phase, the molar fraction of CH₄ is 0.9767, the molar fraction of H₂O is 0.0133, and the molar fraction of CO₂ is 0.01;

② In the liquid phase, the mole fraction of H₂O is 0.9992, the mole fraction of CH₄ is 0.0007, and the mole fraction of CO₂ is 0.0001.

Table 2. Composition of model fluid

Component	CH ₄	CO ₂	H ₂ O
Mole fraction	0.9767	0.01	0.0133

Considering five reactive minerals in sandstone gas reservoirs, the volume fractions of each mineral are shown in Table 3.

Table 3. Mineral volume fraction settings

Mineral	Chemical formula	Volume fraction
Calcite	CaCO ₃	0.0088
Anorthite	CaAl ₂ Si ₂ O ₈	0.0088
K-feldspar	KAlSi ₃ O ₈	0.0176
Kaolinite	Al ₂ Si ₂ O ₅ (OH) ₄	0.029
Illite	K _{0.6} Mg _{0.25} Al _{2.3} Si _{3.5} O ₁₀ (OH) ₂	0.017

The ion content of formation water is shown in Table 4, and the water type is calcium chloride type with a mineralization degree of 20000 mg/L.

Table 4. Ion content of formation water

Ion name	Na ⁺	Ca ²⁺	K ⁺	Mg ²⁺	Cl ⁻	SO ₄ ²⁻	HCO ₃ ⁻
Content/(mg/L)	4060	3070	498	21.7	11805.8	529	15.5

2.2 Simulation Results and Analysis

2.2.1 Pressure Changes During Injection Process

Taking the grid where the Injection well is located as an example, the pressure change with time is analyzed. From Fig. 3, it can be seen that with the continuous injection of CO₂, the grid pressure gradually increases.

2.2.2 CO₂ Dissolution and Water Evaporation Law

The change of CO₂ solubility with time at the grid where the Injection well is located is shown in Fig. 4, from which it can be seen that: with the continuous injection of CO₂, the solubility of CO₂ in water is increasing; And the solubility of CO₂ increases rapidly during the initial injection stage.

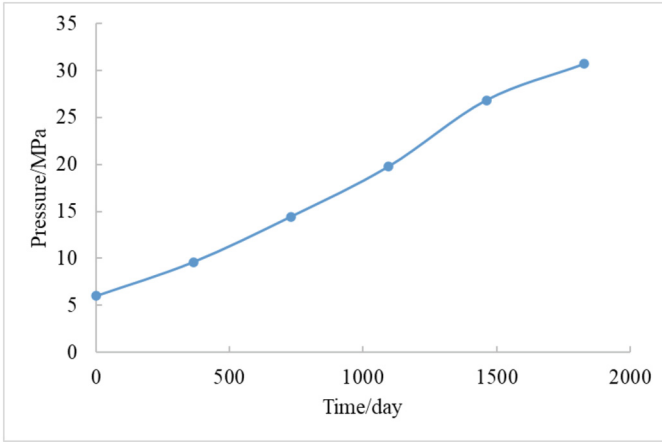


Fig. 3. Pressure variation curve with injection time

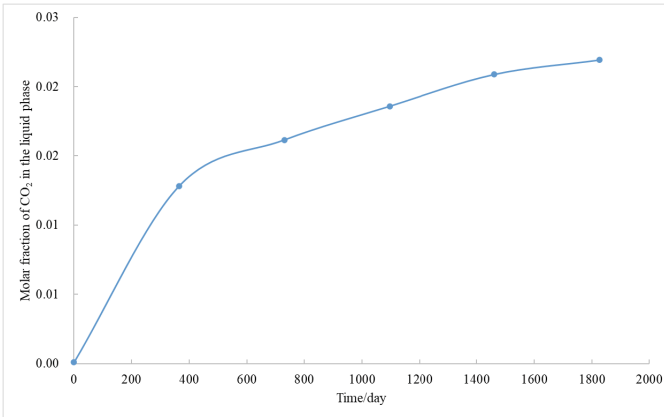


Fig. 4. Change curve of CO₂ molar fraction in liquid phase with injection time

During the injection process, dry CO₂ will continuously evaporate water into the gas phase, resulting in a continuous decrease in the water saturation of the formation. It can be seen from Fig. 5 and Fig. 6 that with the increase in injection time, the mole fraction of H₂O in the gas phase in the grid where the Injection well is located gradually decreases, and the water saturation continuously decreases, indicating that the mole number of H₂O components in the gas phase is increasing.

2.2.3 Mineral Dissolution/Precipitation Patterns and Changes in Ion Content

The dissolution of CO₂ in the formation water increases its acidity, leading to mineral dissolution and precipitation. Taking the grid where the Injection well is located as an example, Fig. 7 shows the content changes of five minerals with injection time, from which it can be seen that calcite, potassium k-feldspar, and anorthite are mainly

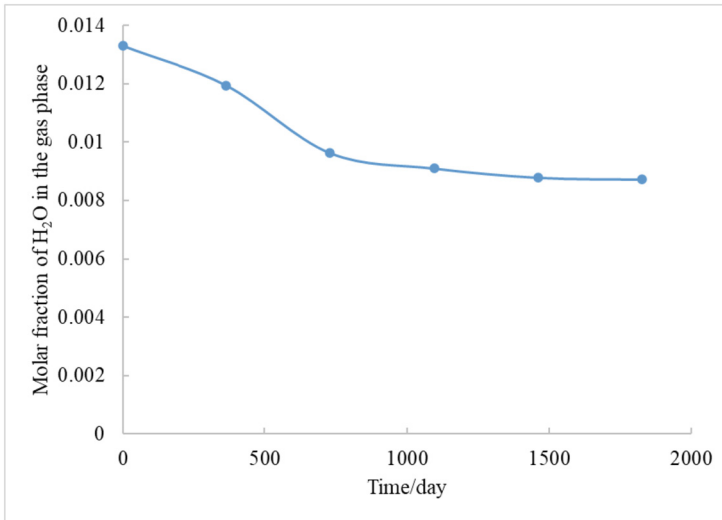


Fig. 5. Variation curve of H₂O molar fraction in gas phase with injection time

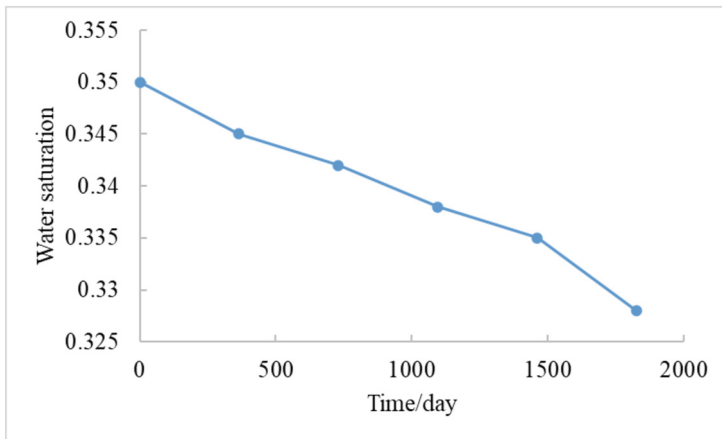


Fig. 6. Water saturation curve with injection time

dissolved, and illite and kaolinite are subject to mineral precipitation. Among them, the dissolution/precipitation amount of calcite, anorthite, and kaolinite changes greatly, while the dissolution/precipitation amount of illite and potassium feldspar is small.

With the injection of CO₂, water evaporation, and salt precipitation, as well as mineral dissolution/precipitation, the ion content of the formation water will continuously change. Figure 8 shows the change of formation water ion molar concentration with injection time at the grid where the Injection well is located. It can be seen from it that with the increase of injection time, the molar concentration of Ca²⁺, HCO₃⁻, H⁺, Al³⁺ and SiO₂(aq) ions increases continuously, while the molar concentration of OH

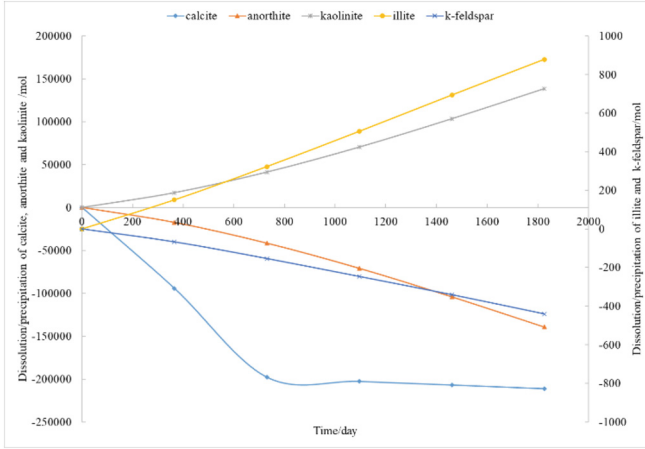


Fig. 7. Curve of mineral dissolution/precipitation amount over time

ions decreases gradually; Moreover, the molar concentrations of Al^{3+} and $SiO_2(aq)$ ions vary little over time. The reason for the analysis is that during the CO_2 injection process, the ionization of carbonate leads to a gradual increase in the molar concentration of H^+ and HCO_3^- ions in the formation of water. The massive dissolution of calcite causes the continuous increase of Ca^{2+} ion concentration in the formation of water. The dissolution of anorthite provides a large amount of Ca^{2+} , Al^{3+} and $SiO_2(aq)$ ions for the solution system, resulting in the precipitation of kaolinite; At the same time, the dissolution/precipitation of illite and k-feldspar minerals will also lead to changes in the content of Al^{3+} and $SiO_2(aq)$ ions in the solution system; Under the combined action of the two, the concentration of Al^{3+} and $SiO_2(aq)$ ions in the formation water slightly increases.

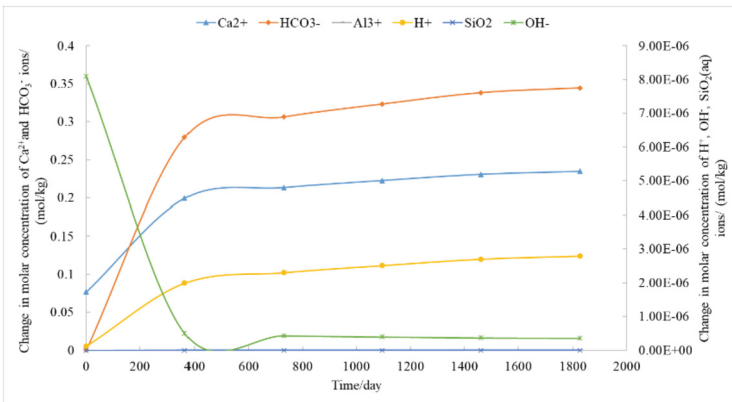


Fig. 8. Curve of ion content in formation water over time

2.2.4 Analysis of Salt Precipitation Law

In theory, the change in pressure during CO₂ injection directly affects the dissolution of CO₂ and the evaporation of water, resulting in mineral dissolution and precipitation, which in turn affects the ion balance and salinity of the formation water, leading to salt precipitation. The following will be analyzed separately:

The effect of water evaporation on salt precipitation

As the water evaporates, the water saturation gradually decreases, leading to a continuous increase in the mineralization degree of the formation of water. Taking the grid where the Injection well is located as an example, it can be seen from Fig. 9 that the salinity of formation water only increased by 1341 mg/L in the whole injection process. The reason is that after five years of continuous CO₂ injection, the water saturation of the grid where the Injection well is located has only decreased by 0.022, so the salinity of formation water has little change, only 6.71%. This indicates that water evaporation has a relatively small impact on the mineralization degree of the formation water.

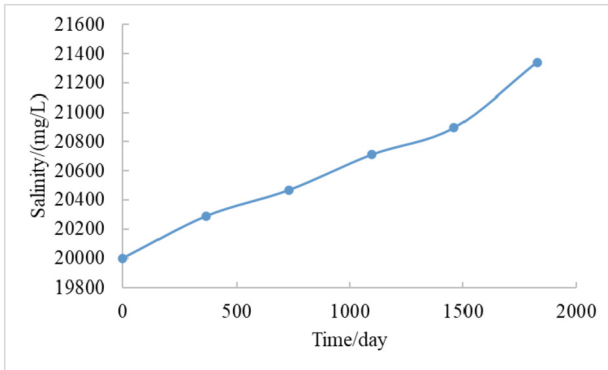


Fig. 9. Variation curve of formation water salinity with injection time

The change in salinity of formation water will cause a change in the saturation index of salt composition. From Fig. 10, it can be seen that due to the small increase in mineralization degree, the saturation index of different salt components varies less. When the mineralization degree increases to 20289 mg/L, the saturation index of CaCO₃ is 0.029; When the mineralization degree increases to 21341 mg/L, the saturation index of CaSO₄ is 0.001. Therefore, as the water evaporates, CaCO₃ and CaSO₄ will separate from the formation water.

② Effect of CO₂ dissolution on salting out

The following will take the formation water data in Table 4 as an example to study the influence of CO₂ dissolution on salting-out during CO₂ injection.

Based on the previous Sect. 1.4, the influence of CO₂ dissolution on the precipitation of CaCO₃, CaSO₄, and CaSO₄·2H₂O was analyzed. The curve of the saturation index with CO₂ solubility is shown in Fig. 11.

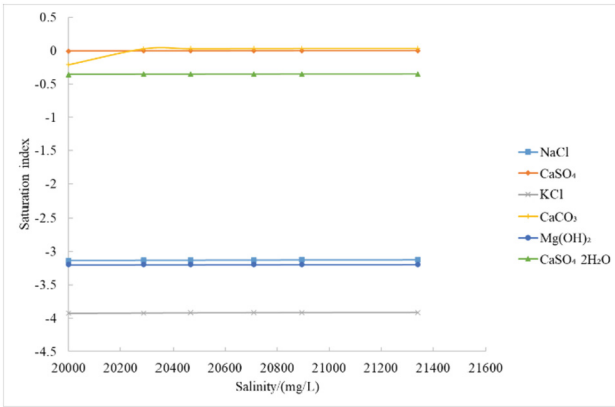


Fig. 10. Variation curve of salt composition saturation index under different salinity

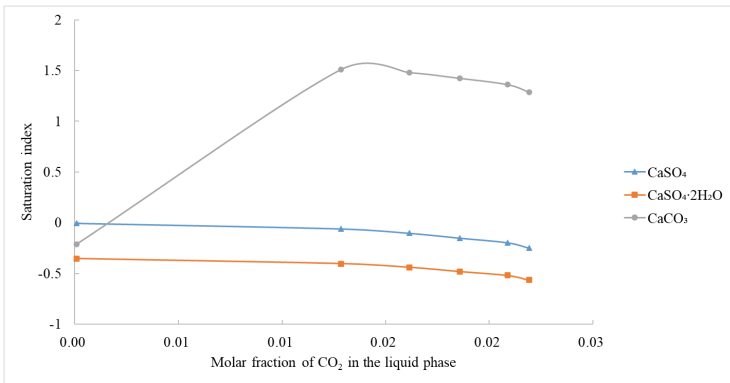


Fig. 11. Variation curve of saturation index of three salt components with CO₂ solubility

From Fig. 11, it can be seen that when considering the effect of CO₂ dissolution on salt precipitation, as the solubility of CO₂ increases, the saturation index of CaCO₃ gradually increases, and CaCO₃ is in a supersaturated state, which will precipitate from the formation water; Meanwhile, the saturation index of the other two salts decreases with the increase of CO₂ solubility. Therefore, the dissolution of CO₂ promotes the precipitation of CaCO₃, while also inhibiting the precipitation of CaSO₄ and CaSO₄·2H₂O.

3 Conclusion

- (1) After the injected CO₂ is dissolved in formation water, it will cause the dissolution of calcite, anorthite, and k-feldspar, as well as the precipitation of illite and kaolinite. Under the combined action of water rock chemical reaction and salt precipitation, the content of OH⁻ ions in the formation water will gradually decrease, while the content of H⁺, Ca²⁺, HCO₃⁻, Al³⁺, SiO₂(aq) ions will continue to increase.

- (2) With the injection of CO₂, the formation pressure increases gradually, and the mole fraction of CO₂ in the water phase increases gradually. Compared with NaCl formation water, the precipitation of CaSO₄ and CaSO₄·2H₂O in CaCl₂ formation water is inhibited, and CaCO₃ is the main product of precipitation.
- (3) During CO₂ injection, water evaporation causes a continuous decrease in formation water saturation, indicating a gradual increase in the mole number of H₂O components in the gas phase. Due to the small decrease in water saturation, the increase in the formation of water mineralization is relatively small, indicating that water evaporation has a relatively small impact on the formation water mineralization.

References

1. Jiang, H., Shen, P., Wang, N., et al.: World carbon dioxide emission reduction policies and prospects for reservoir geological storage. *China Foreign Energy* **05**, 7–13 (2007)
2. Hughes, D.S.: Carbon storage in depleted gas field: key challenges. *Energy Procedia* **1**(1), 3007–3014 (2009)
3. Cui, G., Ren, S., Zhang, L., et al.: Evaporation and saltout rules of formation water in high-temperature gas reservoirs and their impact on productivity. *Pet. Explor. Dev.* **43**(05), 749–757 (2016)
4. Tang, Y., Du, Z., Jiang, H., et al.: Reservoir damage caused by formation water salting out in high-temperature and high-pressure gas reservoirs. *J. Pet.* **33**(05), 859–863 (2012)
5. Tang, Y., Du, Z., Sun, L., et al.: Current status of research on phase behavior and percolation of abnormally high temperature oil and gas reservoirs considering formation water evaporation. *Drill. Prod. Technol.* (05), 82–85+168–169 (2007)
6. Wang, B.: Study on the evaporation and salt deposition of highly mineralized formation water in the near wellbore zone of the gas field. *Southwest Pet. Univ.* (2016)
7. Zhang, G., Taberner, C., Cartwright, L., et al.: Injection of supercritical CO₂ into deep saline carbonate formations: predictions from geochemical modeling. *SPE J.* **16**(4), 959–967 (2011)
8. Peysson, Y.: Permeability alteration induced by drying of brines in porous media. *EPJ Appl. Phys.* **60**(2), 24206 (2012)
9. Lu, H., Yang, H., Moh'd, M.A. et al.: Study on reservoir drying during the injection production cycle of underground gas storage. *Pet. Drill. Technol.* **46**(04), 1–8 (2018)
10. Shen, C., Wang, D., Ren, Z., et al.: Theoretical model and practice of salt deposition in gas wells based on formation water evaporation: a case study of wen 23 gas storage. *Nat. Gas Ind.* **42**(07), 65–74 (2022)
11. Kleinitz, W., Koehler, M., Dietzsch, G.: The precipitation of salt in gas producing wells. In: *SPE European Formation Damage Conference*. Society of Petroleum Engineers (2001)
12. Wang, C., Wu, Y., Wang, Y., et al.: Research progress in formation water evaporation and salting out in porous media. *Appl. Chem. Eng.* **49**(S2), 261–265 (2020)
13. Morin, E., Montel, F.: Accurate predictions for the production of vaporized water. In: *SPE Technical Conference & Exhibition* (1995)
14. Ott, H., Kloe, K.D., Taberner, C., et al.: Rock/fluid interaction by injection of supercritical CO₂/H₂S: investigation of dry-zone formation near the injection well (2010)
15. Kim, M., Sell, A., Sinton, D.: Aquifer-on-a-chip: understanding pore-scale salt precipitation dynamics during CO₂ sequestration. *Lab Chip* **13**(13), 2508–2518 (2013)
16. Miri, R., Noort, R.V., Aagaard, P., et al.: New insights on the physics of salt precipitation during injection of CO₂ into saline aquifers. *Int. J. Greenhouse Gas Control* **43**, 10–21 (2015)

17. Tang, Y., Yang, R., Du, Z., et al.: Experimental study of formation damage caused by complete water vaporization and salt precipitation in sandstone reservoirs. *Transp. Porous Media* **107**(1), 205–218 (2015)
18. Qi, C., Liu, T., Yi, M.: Equation of state for real gases based on helmholtz free energy. *Chem. Equipment Technol.* **43**(04), 21–25 (2022)
19. Li, Y.K., Nghiem, L.X.: Phase equilibria of oil, gas and water/brine mixtures from a cubic equation of state and henry's law. *Can. J. Chem. Eng.* **64**(3), 486–496 (1986)
20. Peng, D.Y., Robinson, D.B.: A new two-constant equation of state. *Ind. Eng. Chem. Res.* **15**(1), 59–64 (1976)
21. Cramer, S.D.: The solubility of methane, carbon dioxide, and oxygen in brines from 0 °C to 300 °C. *Rep. Invest. U.S., Bur. Mines.* **16** (1982)
22. Luo M.: Improvement of SRK equation and its application in phase equilibrium calculation. Tianjin University (2006)
23. Qian, H., Ma, Z., Li, P.: *Hydrogeochemistry*. Geological Publishing House, Beijing (2012)
24. Liu, N.: Study on fluid migration and water rock interaction of CO₂ geological storage in sandstone reservoirs of continental sedimentary basin. China University of Geosciences (2018)
25. Cai, D.: Study on the interaction between CO₂ injection and water/rock mineral in tight sandstone reservoir. Southwest University of Petroleum (2018)
26. Bethke, C.M.: *Geochemical Reaction Modelling*. Oxford University Press, New York (1996)
27. Yang, Y. (ed.): *Physical Chemistry*. Science Press, Beijing (2015)
28. Ye, C., Zheng, M.: Study on the existing forms and saturation indices of chemical components in the water body of Qinghai Gaskule Salt Lake. *Sci. Technol. Bull.* **34**(21), 101–111 (2016)
29. Lin, L., Qin, S., Jian, C., et al.: Comprehensive evaluation on sealing ability of cap layer for reconstruction of depleted gas reservoir: a case study of Xu-2 Gas reservoir in Zhongba Gas field, Northwest Sichuan. *Pet. Geol. Oilfield Dev. Daqing* **41**(06), 42–50 (2022)
30. Deng, X.: Acidizing technology practice of Zhongbaoxu 2 Gas reservoir. Southwest Petroleum University (2016)
31. Van Genuchten, M.T.: A closed-form equation for predicting the hydraulic conductivity of unsaturated soils. *Soil Sci. Soc. Am. J.* **44**(05), 892–898 (1980)
32. Corey, A.T.: The interrelation between gas and oil relative permeabilities. *Producers Monthly* **19**(1), 38–41 (1954)